

# Primordial perturbations generated by Higgs and $R^2$

Yun-Chao Wang<sup>1</sup> and Tower Wang<sup>1,\*</sup>

<sup>1</sup>*Department of Physics, East China Normal University,  
Shanghai 200241, China*

(Dated: February 9, 2019)

If the very early Universe is dominated by the non-minimally coupled Higgs field and Starobinsky's curvature-squared term together, the potential diagram would mimic the landscape of a valley, serving as a cosmological attractor. The inflationary dynamics along this valley is studied, model parameters are constrained against observational data, and the isocurvature perturbation is evaluated,

## I. INTRODUCTION

Recent observations of the cosmic microwave background radiation [1–3] have acquired more information about the very early Universe. They focused our attention on a smaller region in the  $(n_s, r)$  plane, where  $n_s$  is the scalar spectral index and  $r$  is the tensor-to-scalar ratio, thus giving us more clues to the standard model of slow-roll single-field inflation. Meanwhile, the data also shrunk the parameter space of signatures of new physics, such as the power spectral features, the primordial non-Gaussianities, the residual isocurvature modes, the power asymmetry and the running of spectral index, therefore placing stringent constraints on more complicated inflationary models.

Among typical single-field models of slow-roll inflation, two thrifty models become favored by data and popular recently: the Starobinsky's  $R^2$  inflation [4, 5] and the non-minimally coupled Higgs inflation [6]. In Ref. [4], the  $R^2$  cosmological model was proposed to get a nonsingular isotropic homogeneous picture of the Universe. As a solution to the horizon and flatness problems, the inflationary universe scenario [7–9] is realized often by a scalar field. Both of them are able to generate a perturbation spectrum which may lead to the microwave background anisotropy and the structure formation in the Universe. Interestingly, in the absence of matter, the Starobinsky model is conformally equivalent to the Einstein gravity plus a scalar field [10]. In the same case, it is also equivalent to the large-field model of non-minimally coupled Higgs inflation [6, 11]. Nevertheless, the  $R^2$  inflation and the Higgs inflation can be distinguished observationally by considering their post-inflationary interactions with matter fields [12].

When both a scalar field and a curvature-squared term are effective in driving inflation, inflationary dynamics will be more complicated. To the best of our knowledge, the exploration of such models dates back to three decades ago [13–16]. For instance, Ref. [16] analyzed a specific model of this type where the scalar potential is of the quadratic form. It was found that, in certain conditions, the model can generate two consecutive inflationary stages and a break in the perturbation spectrum. In recent years, there are reviving interests in this class of models, with attention turned to the case of a single inflationary phase, see Refs. [17–21] as a partial list. The model of Ref. [16] was revisited in Ref. [17] under the approximation (10) therein, and in Ref. [18] to the second order in slow-roll parameters. In Refs. [19, 20], inflationary cosmology has been explored in a theory of two scalar fields non-minimally coupled to the Ricci scalar with an extra  $R^2$  term. In Ref. [21], the special case with  $V_H = 0$  was studied analytically and numerically.

In contrast, if one assumes that the Higgs field takes a small value in the very early Universe, then the  $R^2$  term is effective in driving inflation. For this case, it was argued in Ref. [22] that a non-minimal coupling of Higgs field to curvature could alleviate fine-tuning problems of the initial Higgs value, and it was shown in Ref. [23] that the Higgs boson can create a large Wilson coefficient for the  $R^2$  operator.

In this paper, we will study the inflationary dynamics driven by the  $R^2$  term together with a non-minimally coupled Higgs field. In Sec. II, we will write this model in the Einstein frame and illustrate the valley-like potential landscape. In Sec. III, slow-roll inflation in the valley will be analyzed with a single-field approximation and constrained with Planck 2015 data. In Sec. IV, we will perform a two-field numerical simulation validating the single-field approximation. A few subtle points of this model will be discussed in Sec. V.

Throughout this paper,  $M_p = (8\pi G)^{-1/2}$  is the reduced Plank mass. Metric and the Ricci tensor are denoted by  $g_{\mu\nu}$ ,  $R_{\mu\nu}$  in the Jordan frame, and  $\tilde{g}_{\mu\nu}$ ,  $\tilde{R}_{\mu\nu}$  in the Einstein frame.

---

\* Electronic address: twang@phy.ecnu.edu.cn

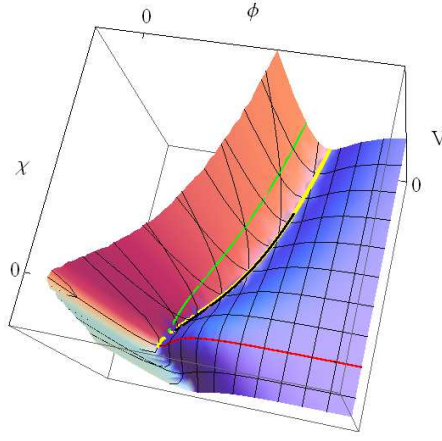


Figure 1. (color online). The 3D diagram of potential (2). We set concretely  $\lambda = 3M^2\xi^2/M_p^2$  here, but the valley-like landscape is robust to parameter variation. Green, red, yellow trajectories are drawn respectively from Eqs. (4), (5), (6). The black thick line in the valley is the field trajectory simulated numerically in Sec. IV from equations of motion.

## II. BIRD VIEW

The full action of Higgs inflation model [6] augmented with an  $R^2$  term can be written as

$$\begin{aligned} \mathcal{S} &= \int d^4x \sqrt{-g} \left[ \frac{M_p^2}{2} R + \frac{1}{2} \xi \chi^2 R + \frac{M_p^2}{12M^2} R^2 - \frac{1}{2} g^{\mu\nu} \partial_\mu \chi \partial_\nu \chi - \frac{1}{4} \lambda \chi^4 \right] \\ &= \int d^4x \sqrt{-\tilde{g}} \left[ \frac{M_p^2}{2} \tilde{R} - \frac{1}{2} \tilde{g}^{\mu\nu} \partial_\mu \phi \partial_\nu \phi - \frac{1}{2} e^{-\sqrt{\frac{2}{3}}\phi/M_p} \tilde{g}^{\mu\nu} \partial_\mu \chi \partial_\nu \chi - V(\phi, \chi) \right], \end{aligned} \quad (1)$$

where the potential in Einstein frame is

$$V(\phi, \chi) = \frac{3}{4} M_p^2 M^2 e^{-2\sqrt{\frac{2}{3}}\phi/M_p} \left( e^{\sqrt{\frac{2}{3}}\phi/M_p} - 1 - \frac{1}{M_p^2} \xi \chi^2 \right)^2 + \frac{1}{4} \lambda \chi^4 e^{-2\sqrt{\frac{2}{3}}\phi/M_p}. \quad (2)$$

The Jordan and Einstein frames are related by the conformal transformation  $\tilde{g}_{\mu\nu} = F g_{\mu\nu}$  with

$$F = 1 + \frac{1}{M_p^2} \xi \chi^2 + \frac{1}{3M^2} R = e^{\sqrt{\frac{2}{3}}\phi/M_p}. \quad (3)$$

This model provides a unification of the Starobinsky inflation and Higgs inflation. One can go back to the Higgs model by imposing the constraint

$$e^{\sqrt{\frac{2}{3}}\phi/M_p} = 1 + \frac{1}{M_p^2} \xi \chi^2 \quad (4)$$

and the Starobinsky model by

$$\chi = 0. \quad (5)$$

To get a bird view, we present a 3D diagram of potential (2) in Fig. 1. It mimics a valley landscape. On the steep side of the valley, the trajectory of Higgs inflation (4) is highlighted with a green line like a thin stratum in the cliff. On the other side, the trajectory of Starobinsky inflation (5) is marked with a red curve along the convex bank akin to a point bar. According to these features in the landscape, we can name the green trajectory (4) as Higgs stratum, and the red trajectory (5) as Starobinsky bar. Apparently, in the full landscape neither the Higgs stratum nor the Starobinsky bar is an attractive track to run inflation. Instead, the valley itself can serve as a natural route for inflatons.

In the following, we will locate the valley and study inflationary dynamics along it. Since the potential possesses a reflection symmetry under  $\chi \leftrightarrow -\chi$ , we will focus on the case  $\chi > 0$  without loss of generality.

### III. INFLATION ALONG THE VALLEY

Model (1) is a good example of non-canonical two-field inflation, which can be handled numerically or semi-analytically along the way of Refs. [24–26]. However, we will take a shortcut in this section. The two-field treatment will be postponed to the next section.

From Fig. 1, we observe that the potential energy changes smoothly in  $\chi$ -direction and violently in  $\phi$ -direction. Or intuitively, the valley extends mainly along  $\chi$ -direction. Therefore, the location of valley can be well estimated by  $V_\phi = 0$ , that is

$$e^{\sqrt{\frac{2}{3}}\phi/M_p} = 1 + \frac{1}{M_p^2}\xi\chi^2 + \frac{1}{3M_p^2M^2}\lambda\chi^4 \left(1 + \frac{1}{M_p^2}\xi\chi^2\right)^{-1}. \quad (6)$$

If inflatons roll in this valley with a negligible isocurvature perturbation, we can substitute this equation into action (1) to eliminate the dependence on  $\phi$ . For small values of  $\chi$ , we obtain

$$\mathcal{S} \approx \int d^4x \sqrt{-\tilde{g}} \left[ \frac{M_p^2}{2} \tilde{R} - \frac{1}{2} \tilde{g}^{\mu\nu} \partial_\mu \chi \partial_\nu \chi - \frac{1}{4} \lambda \chi^4 \right] \quad (7)$$

which cannot support slow-roll inflation. In the regime of large  $\chi$ , we get

$$\begin{aligned} \mathcal{S} \approx \int d^4x \sqrt{-\tilde{g}} \left\{ \frac{M_p^2}{2} \tilde{R} - \frac{M_p^2}{2} \frac{1}{\chi^2} \left[ 6 + \frac{1}{\xi} \left( 1 + \frac{M_p^2}{3M^2} \frac{\lambda}{\xi^2} \right)^{-1} \right] \tilde{g}^{\mu\nu} \partial_\mu \chi \partial_\nu \chi \right. \\ \left. - \frac{M_p^4}{4} \frac{\lambda}{\xi^2} \left( 1 + \frac{M_p^2}{3M^2} \frac{\lambda}{\xi^2} \right)^{-1} \left[ 1 - \frac{2M_p^2}{\xi\chi^2} \left( 1 + \frac{M_p^2}{3M^2} \frac{\lambda}{\xi^2} \right)^{-1} \right] \right\}. \quad (8) \end{aligned}$$

Presuming  $\lambda > 0$  and  $\xi > 0$ , the large- $\chi$  section of the valley is suitable for driving inflation. To see this, we rewrite action (8) in the kinetic formulation [27] as

$$\mathcal{S} = \int d^4x \sqrt{-\tilde{g}} \left[ \frac{M_p^2}{2} \tilde{R} - \frac{M_p^2}{2} \left( \frac{a}{\rho^2} + \dots \right) \tilde{g}^{\mu\nu} \partial_\mu \rho \partial_\nu \rho - V_0 (1 - c\rho + \dots) \right], \quad (9)$$

where  $\rho = \chi^{-2}$  and

$$\begin{aligned} V_0 &= \frac{M_p^4}{4} \frac{\lambda}{\xi^2} \left( 1 + \frac{M_p^2}{3M^2} \frac{\lambda}{\xi^2} \right)^{-1}, \\ a &= \frac{3}{2} + \frac{1}{4\xi} \left( 1 + \frac{M_p^2}{3M^2} \frac{\lambda}{\xi^2} \right)^{-1}, \\ c &= \frac{2M_p^2}{\xi} \left( 1 + \frac{M_p^2}{3M^2} \frac{\lambda}{\xi^2} \right)^{-1}. \quad (10) \end{aligned}$$

Following Ref. [27], one can calculate the scalar spectral index and tensor-to-scalar ratio at the leading order in  $1/N$ ,

$$n_s = 1 - \frac{2}{N}, \quad r = \frac{12}{N^2} \left[ 1 + \frac{1}{6\xi} \left( 1 + \frac{M_p^2}{3M^2} \frac{\lambda}{\xi^2} \right)^{-1} \right]. \quad (11)$$

This suggests that the model has the same behavior as  $\alpha$ -attractors [28–30] with

$$\alpha = 1 + \frac{1}{6\xi} \left( 1 + \frac{M_p^2}{3M^2} \frac{\lambda}{\xi^2} \right)^{-1}. \quad (12)$$

After straightforward calculations, we find the leading-order amplitude of curvature power spectrum is

$$A_s = \frac{N^2}{12\pi^2} \left( \frac{\xi}{\lambda} + \frac{6\xi^2}{\lambda} + \frac{2M_p^2}{M^2} \right)^{-1}. \quad (13)$$

Cosmological parameter		Model parameter	
$n_s$	$0.9677 \pm 0.0060$	$N$	61.9
$10^9 A_s$	$2.139 \pm 0.063$	$\frac{\xi}{\lambda} + \frac{6\xi^2}{\lambda} + \frac{2M_p^2}{M^2}$	$1.51 \times 10^{10}$
$r_{0.002}$	$< 0.114$	$6\xi + \frac{2M_p^2}{M^2} \frac{\lambda}{\xi}$	$> 0.0282$

Table I. The 68% C.L. limits on  $n_s$ ,  $A_s$  and the 95% C.L. limit on  $r_{0.002}$  from Planck 2015 results [2] and the derived best-fit value of model parameters.

Eqs. (11), (13) connect parameters of the model to cosmological parameters. Accordingly the best-fit value of cosmological parameters can be used to estimate model parameters. In Table I, we confront this model with Planck 2015 constraints [2]. One can deduce that  $\xi/\lambda < 1.47 \times 10^{10}$  and hence

$$\frac{3\xi^2}{\lambda} + \frac{M_p^2}{M^2} > 0.02 \times 10^{10}. \quad (14)$$

As indicated by this bound, fine-tuning is unavoidable in viable models of this class. One has to tune either the Higgs couplings just as usually done in Higgs inflation model, or the coefficient of  $R^2$  term like Starobinsky model. Or both.

We mention two special cases in passing. First, in the limit  $M_p^2/M^2 \rightarrow 0$ , if  $\xi \gg 1$ , then Eqs. (11), (13) tend to the results of Higgs model,

$$n_s = 1 - \frac{2}{N}, \quad r = \frac{12}{N^2}, \quad A_s = \frac{N^2}{72\pi^2 M_p^2} \frac{\lambda}{\xi^2}. \quad (15)$$

Second, for the special case  $\xi = 0$ , parallel calculations with  $\rho = \chi^{-4}$  yield

$$n_s = 1 - \frac{2}{N}, \quad r = \frac{12}{N^2}, \quad A_s = \frac{N^2 M^2}{24\pi^2 M_p^2}. \quad (16)$$

This is the same as the predictions of Starobinsky model.

#### IV. ISOCURVATURE PERTURBATION

In the previous section, by inserting Eq. (6) into the action, we have implicitly assumed that both background fields and their perturbations evolve along the valley. This means we have ignored isocurvature perturbation transverse to the valley. Through numerical simulations, here we will show that the isocurvature perturbation is indeed ignorable in contrast to curvature perturbation.

To run the numerical algorithm, we should assign the values of model parameters, the initial values and initial velocities of fields. On the one hand, the initial value of  $\chi$  is related to e-folding number by

$$N = \frac{1}{8M_p^2} \chi_*^2 \left( 1 + 6\xi + \frac{2M_p^2}{M^2} \frac{\lambda}{\xi} \right). \quad (17)$$

Given model parameters, one can determine the initial values of  $\chi$ ,  $\phi$  from this relation and the equation of valley (6). Then the initial velocities  $\dot{\chi}$ ,  $\dot{\phi}$  can be derived from the equations of motion in slow roll. On the other hand, the inflation model involves four parameters  $N$ ,  $M$ ,  $\lambda$ ,  $\xi$  constrained by two equalities and one inequality in table I. Therefore, two more equalities are in demand. In our numerical simulations, we will set the tensor-to-scalar ratio to a moderate value  $r = 0.05$  and assume that the two terms on the left hand side of (14) contribute equally  $\lambda = 3M^2\xi^2/M_p^2$ .

After setting model parameters and initial conditions above, we run our numerical algorithm as in Ref. [26] and generate the power spectra in Fig. 2. In the right panel, it is clear that the isocurvature perturbation is significantly suppressed and decaying in the epoch of inflation. This is in accordance with our single-field approximation in Sec. III. The spectral index can be inferred from the left panel,  $n_s - 1 = d \ln(\mathcal{P}_{\mathcal{R}}/\mathcal{P}_{\mathcal{R}*})/d \ln(k/k_*) \approx (-0.8 \ln 10)/N \approx -1.8/N$ , roughly agreeing with the leading-order result (11).

The trajectory of fields  $\chi$ ,  $\phi$  is also simulated, see the black thick line in Fig. 1. It is indistinguishable from the yellow line drawn from Eq. (6).

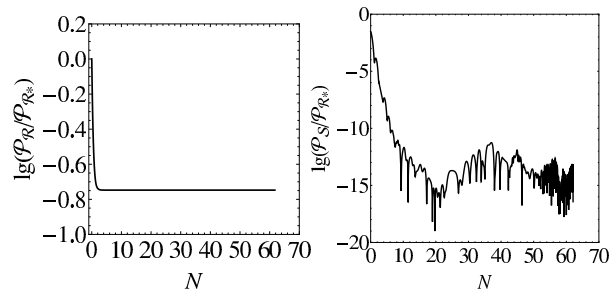


Figure 2. The power spectra of curvature perturbation (left panel) and isocurvature perturbation (right panel). Initial conditions and model parameters are assigned in Sec. IV.

## V. DISCUSSION

Combining the Higgs inflation model and the Starobinsky's  $R^2$  inflation model together, we have found that there is a cosmological attractor for inflation. It is situated in a valley of the potential landscape, deviating often from both the Higgs inflation trajectory and the Starobinsky inflation trajectory. Along the valley, slow-roll inflation takes place in the large field regime. The single-field approximation is powerful in analyzing this model and predicts  $n_s$ ,  $r$  with similar behaviors to  $\alpha$ -attractors.

In plotting Fig. 2, we have assumed  $\lambda \sim 3M^2\xi^2/M_p^2$ , that is, the two terms are of the same order on the left hand side of (14). Otherwise, if the first term dominates,  $\lambda \ll 3M^2\xi^2/M_p^2$ , the cliff will be straight, and the yellow line will overlap with the green line, restoring Higgs inflation. When the second term dominates,  $\lambda \gg 3M^2\xi^2/M_p^2$ , the valley will form a deep V around the Starobinsky bar, and the yellow line will approach the red curve, recovering Starobinsky inflation.

In two-field inflation models, the isocurvature perturbation usually works as a source term for curvature perturbation on super-horizon scales. In this paper, such effects are suppressed by restricting inflatons to the valley, or technically, by putting inflatons at a slow-roll position inside the valley initially. With initial conditions of this sort, the single-field approximation is valid. It would be interesting to go beyond the single-field approximation by starting with different initial conditions.

## ACKNOWLEDGMENTS

This work is supported by the National Natural Science Foundation of China (Grant Nos. 11105053 and 91536218).

- 
- [1] P. A. R. Ade *et al.* [BICEP2 and Planck Collaborations], Phys. Rev. Lett. **114**, 101301 (2015) [arXiv:1502.00612 [astro-ph.CO]].
  - [2] P. A. R. Ade *et al.* [Planck Collaboration], Astron. Astrophys. **594**, A13 (2016) [arXiv:1502.01589 [astro-ph.CO]].
  - [3] P. A. R. Ade *et al.* [Planck Collaboration], Astron. Astrophys. **594**, A20 (2016) [arXiv:1502.02114 [astro-ph.CO]].
  - [4] A. A. Starobinsky, Phys. Lett. B **91**, 99 (1980).
  - [5] A. A. Starobinsky, Sov. Astron. Lett. **9**, 302 (1983).
  - [6] F. L. Bezrukov and M. Shaposhnikov, Phys. Lett. B **659**, 703 (2008) [arXiv:0710.3755 [hep-th]].
  - [7] A. H. Guth, Phys. Rev. D **23**, 347 (1981).
  - [8] A. D. Linde, Phys. Lett. B **108**, 389 (1982).
  - [9] A. Albrecht and P. J. Steinhardt, Phys. Rev. Lett. **48**, 1220 (1982).
  - [10] B. Whitt, Phys. Lett. B **145**, 176 (1984).
  - [11] A. Kehagias, A. M. Dizgah and A. Riotto, Phys. Rev. D **89**, no. 4, 043527 (2014) [arXiv:1312.1155 [hep-th]].
  - [12] F. L. Bezrukov and D. S. Gorbunov, Phys. Lett. B **713**, 365 (2012) [arXiv:1111.4397 [hep-ph]].
  - [13] L. A. Kofman, A. D. Linde and A. A. Starobinsky, Phys. Lett. B **157**, 361 (1985).
  - [14] A. A. Starobinsky, JETP Lett. **42**, 152 (1985) [Pisma Zh. Eksp. Teor. Fiz. **42**, 124 (1985)].
  - [15] V. Muller and H. J. Schmidt, Gen. Rel. Grav. **21**, 489 (1989).
  - [16] S. Gottlober, V. Muller and A. A. Starobinsky, Phys. Rev. D **43**, 2510 (1991).
  - [17] V. H. Cardenas, S. del Campo and R. Herrera, Mod. Phys. Lett. A **18**, 2039 (2003) [gr-qc/0308040].
  - [18] C. van de Bruck and L. E. Paduraru, Phys. Rev. D **92**, 083513 (2015) [arXiv:1505.01727 [hep-th]].
  - [19] K. Bamba, S. D. Odintsov and P. V. Tretyakov, Eur. Phys. J. C **75**, no. 7, 344 (2015) [arXiv:1505.00854 [hep-th]].
  - [20] K. Bamba, arXiv:1602.08911 [hep-th].
  - [21] S. Kaneda and S. V. Ketov, Eur. Phys. J. C **76**, no. 1, 26 (2016) [arXiv:1510.03524 [hep-th]].
  - [22] M. Torabian, arXiv:1410.1744 [hep-ph].
  - [23] X. Calmet and I. Kuntz, Eur. Phys. J. C **76**, no. 5, 289 (2016) [arXiv:1605.02236 [hep-th]].

- [24] D. Langlois, Phys. Rev. D **59**, 123512 (1999) [astro-ph/9906080].
- [25] C. van de Bruck and M. Robinson, JCAP **1408**, 024 (2014) [arXiv:1404.7806 [astro-ph.CO]].
- [26] Y. C. Wang and T. Wang, arXiv:1603.09567 [gr-qc].
- [27] M. Galante, R. Kallosh, A. Linde and D. Roest, Phys. Rev. Lett. **114**, no. 14, 141302 (2015) [arXiv:1412.3797 [hep-th]].
- [28] S. Ferrara, R. Kallosh, A. Linde and M. Porrati, Phys. Rev. D **88**, no. 8, 085038 (2013) [arXiv:1307.7696 [hep-th]].
- [29] R. Kallosh, A. Linde and D. Roest, JHEP **1311**, 198 (2013) [arXiv:1311.0472 [hep-th]].
- [30] A. Linde, JCAP **1505**, 003 (2015) [arXiv:1504.00663 [hep-th]].